The 260-W coherent beam combining of two compact fibre amplifier chains*

Wang Xiao-Lin(王小林)[a)†], Ma Yan-Xing(马阎星)[a)], Zhou Pu(周 朴)[a)], He Bing(何 兵)[b)], Xue Yu-Hao(薛宇豪)[b)], Liu Chi(刘 驰)[b)], Li Zhen(李 震)[b)], Xiao Hu(肖 虎)[a)], Xu Xiao-Jun(许晓军)[a)], Zhou Jun(周 军)[b)], Liu Ze-Jin(刘泽金)[a)], and Zhao Yi-Jun(赵伊君)[a)]

[a)] *College of Optoelectronic Science and Engineering, National University of Defense Technology, Changsha* 410073, *China*

[b)] *Shanghai Institute of Optics and Fine Mechanics, Shanghai* 201800, *China*

(Received 21 February 2011; revised manuscript received 11 June 2011)

Coherent beam combining of two fibre amplifier chains with a total power of 260 W in a compact system using the stochastic parallel gradient descent (SPGD) algorithm is demonstrated. A 150 MHz linewidth fibre laser is built and introduced for high-power amplification to mitigate stimulated Brillouin scattering (SBS). Compact high-power amplifier chains are built with low power all-fibre system and high-power bulk free-optics fibre amplifiers. When the total power is about 260 W, active phase-locking of two high-power amplifiers is demonstrated using the SPGD algorithm. In closed-loop, the power in the main lobe increases 1.68 times, the visibility is increased from 0 to 0.62, and the phase residual error is less than $\lambda/10$.

Keywords: fibre amplifier, coherent beam combining, stimulated Brillouin scattering, stochastic parallel gradient descent algorithm

PACS: 42.25.Kb, 42.55.Wd, 42.65.Es **DOI:** 10.1088/1674-1056/20/11/114203

1. Introduction

Coherent beam combining (CBC) of fibre lasers provides a versatile way to scale up laser power with good beam quality as fibre laser power scaling is restricted in by the thermal load, fibre damage, and nonlinear effect. Up to now, there are three main configurations for CBC, including passive phasing,[1−3] active phasing configuration,[4−7] and hybrid phasing.[8] Master oscillator power amplifier (MOPA) based active phasing is the most effective way for CBC.[4,6,9] In this configuration, single frequency seed laser is often considered to be necessary to improve the spatial coherence property and obtain high brightness in the far-field.[10] However, the output power of the single frequency amplifier is about hundreds of watts level as restricted by the nonlinear effects, especially the stimulated Brillouin scattering (SBS).[11,12] This is also a great challenge to the increase of the total power of CBC. In this paper, in order to suppress the SBS and scale up to a high power, we introduce a quasi-single frequency laser with a linewidth of 150 MHz for power amplification. In the four main active phase control techniques, digital holography technique,[13] heterodyne phase detection technique,[14] multi-dither technique,[15,16] and stochastic parallel gradient descent (SPGD) algorithm technique,[17,18] the SPGD algorithm may be the most attractive one due to its advantage of being mode-free, simple to implement and ease of constructing a compact system. For the same reason, CBC using SPGD algorithm has been proposed to build new architecture of high energy laser system, adaptive photonics phase-locked elements (APPLE).[19] However, so far, the power demonstration of CBC using SPGD algorithm is only about 73.5 W.[20] In this paper, we will demonstrate CBC of two compact fibre amplifier chains with a total power as high as 260 W by using SPGD algorithm for the first time to our knowledge, and the stability and expansibility of the SPGD algorithm is demonstrated again.

2. Experimental setup

The experimental setup is shown in Fig. 1. The master oscillator (MO) is a home-made linearly polarized single-longitudinal mode laser, generating 10 mW

*Project supported by the Innovation Foundation for Graduates in National University of Defense Technology, China (Grant No. B080702).

†Corresponding author. E-mail: wxllin@nudt.edu.cn

© 2011 Chinese Physical Society and IOP Publishing Ltd

of power at a wavelength of about 1064.4 nm with a linewidth of 150 MHz. The MO is first preamplified to 100 mW, then split into four channels and two of them are coupled into two phase modulators (PM, NIR-MPX-LN-0.1-P-P-FA-FA, Photoline inc., half voltage 2.2 V, insert loss 3.0 dB). Each laser beam from the PM is coupled into an amplifier chain and is amplified from 10 mW to more than 130 W. Laser beams from power amplifiers are collimated by specially designed large-diameter collimators (CO) with a diameter of about 6.5 mm. Positions of the collimators are carefully tuned to ensure laser beams to be precisely arranged with high fill factor. The fill factor is defined as the beam width divided by the distance between the adjacent beams. In the experiment, the fill factor of the near-field laser array is calculated to be 56%. In the free space, simulated turbulences are induced by round-the-clock working cooling fans and air-conditioners in the clean-room laboratory. The main power (∼99% power) of the combined beam transmit after a sampler mirror (BS1) is sent to a power meter, the reflected beam (∼1% power) is used for profile diagnosis and active phase control. A lens is used to simulate the far-field pattern and then a sampler is located behind the lens. The reflected beam from the sampler (BS2) is sent into an infrared camera (SP620U, Ophir-spiricon inc.) for profile diagnose. The transmission beam from the sampler is sent into the end of a single mode (SM) fibre (Corning HI 1060, 5.3 μm core diameter, 0.14 NA@1064 nm). The SM fibre is 0° cleaved and used to collect the power of the main lobe of the far-field interference pattern.[18,21]. The output power of the SM fibre laser is sent into a photodetector (PD, PDA36A-EC, Thorlabs). The location of the SM fibre is carefully adjusted to ensure the maximum output signal of the detector. The optical power detected by the photoelectric detector is defined as the metric function J, which is shared by the oscilloscope and the algorithmic controller. In our experiment, SPGD algorithm is performed on the digital signal processor (DSP, TMS320C6713, TI inc.) based algorithmic controller. Phase control signals are generated by the DSP and sent to the phase modulators through digital to analogy (D/A) converters. The update rate of the SPGD controller is more than 100000 iterations per second, the phase-locking compensation bandwidth is higher than 2 kHz in two laser beam combining.[22]

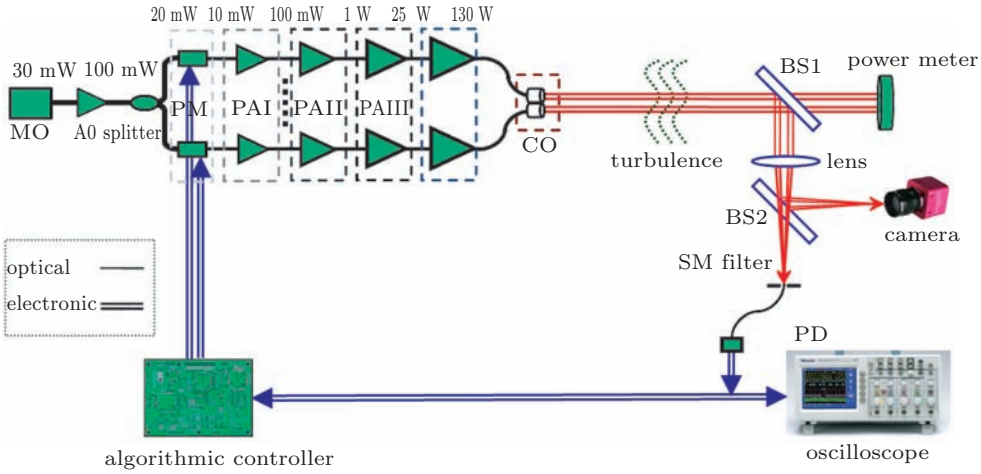


Fig. 1. (colour online) Experimental setup for high power high fill factor CBC.

In the present experiment, in order to mitigate SBS and improve the power of the amplifier, a homemade fibre laser with a linewidth of about 150 MHz is used as a master oscillator. The spectrum and longitudinal mode characteristics are measured by optical spectrum analyser (Agilent 86140B) and Fabry–Pérot interferometer (Topica FPI100, 1 GHz free spectral range) respectively. The measured centre wavelength is about 1064.4 nm and the linewidth is about 150 MHz, as shown in Fig. 2. Although a linewidth of about 150 MHz is not broad enough to suppress the SBS completely, the SBS can be mitigated a lot compared with a 10 kHz linewidth single-frequency seed laser. The wide linewidth (∼ 150 MHz) also means a short coherence length (∼ 2 m), so the optical path difference should be controlled to less than 0.5 m to

ensure a high visibility interference pattern. In our experiment, the optical path difference can be easily controlled to less than 0.1 m by cutting and fusing of fibres as well as tuning the position of collimators in free space optical path.

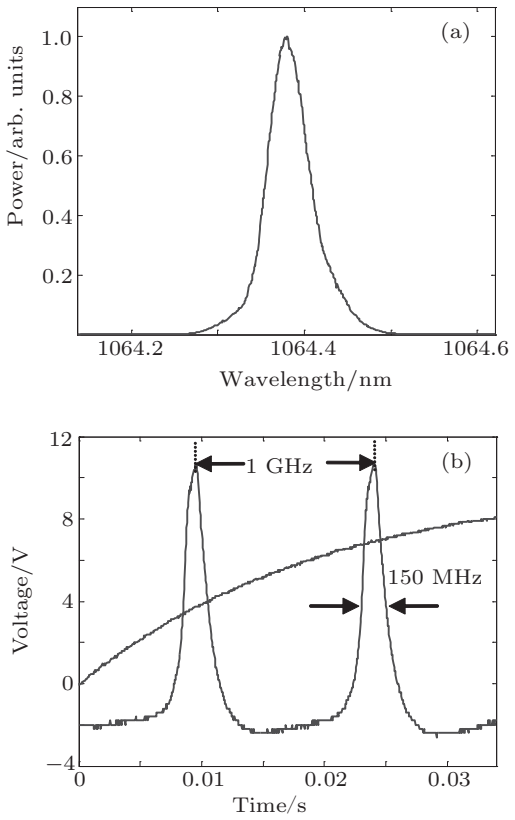


Fig. 2. (a) Optical spectrum and (b) oscilloscope trace of Fabry-Pérot of the home-made MO.

Each high-power amplifier chain consists of three low-power all-fibre amplifiers combined with high-power spatial configuration based amplifier, as shown in Fig. 3. The first three stage amplifiers (PAI, PAII and PAIII in Fig. 1) are specially designed with polarization maintained all-fibre components, which makes the system compact. The main power amplifiers (PAIV) are bulk free-optics fibre amplifiers and non-polarization-maintained. The main amplifier is based on a $\sim$ 12 m long large-mode area (LMA) SM ytterbium-doped fibre (YDF) for high power operation. The LMA fibre has a 30 μm diameter core with numerical aperture (NA) 0.08 and the inner cladding diameter is 400 μm with NA 0.46. A compact pump and signal coupling system is designed for high-precision and coupling efficiency, as shown in Fig. 3. Both ends of the active fibre are polished at an angle of about 8° to suppress spurious lasing as a result of Fresnel reflections. The output end of the fibre is directly inserted into the specially designed large-diameter collimators and the collimated beam with a diameter of about 6.5 mm is sent to the free space. Backward laser beams from the main amplifier is sampled and collected by a sampler and a focus lens. The collected beam is sent to an optical spectrum analyser (OSA) to monitor the SBS. In the experiment, two amplifiers are pumped by a single fibre coupled diode laser bars. The pump beam is split into two beams which are sent to the amplifiers separately.

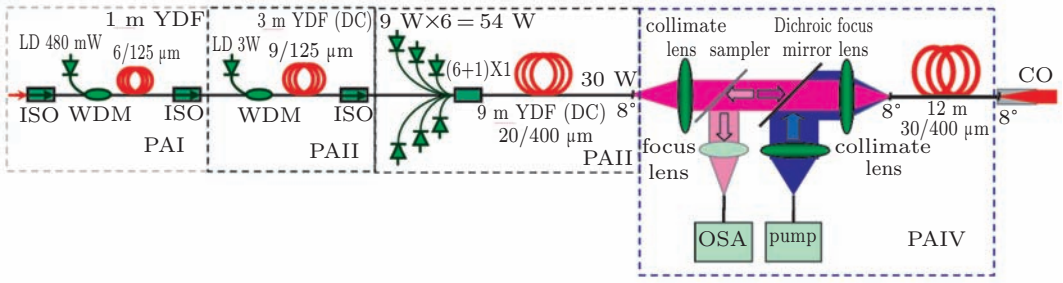


Fig. 3. (colour online) Configuration of the power amplifier chain. PAI, PAII, PAIII, PIV are amplifiers in different stages; ISO: isolator; LD: Laser diode; WDM: wavelength division multiplexer; YDF: Yb^{3+} doped fibre; DC: double cladding; OSA: optical spectrum analyser.

In active phase control, the SPGD algorithm can be briefly described as follows.[18] The metric function $J = J(\boldsymbol{u})$ is a function of $\boldsymbol{u}$, where $\boldsymbol{u} = (u_1, \ldots, u_j, \ldots, u_N)$, with u_j being the control signal applied to the $LiNbO_3$ phase modulator. The algorithm is implemented in infinite iterations until ended manually. Each iteration cycle works as follows:

(i) Generate statistically independent random perturbations and convert them to voltages $\delta\boldsymbol{u} = \{\delta u_1, \delta u_2, \ldots, \delta u_N\}$, where all $|\delta u_i|$ are small values that are typically chosen as statistically independent variables having zero mean and equal variances, $\langle \delta u_k \rangle = 0$, $\langle \delta u_k \delta u_l \rangle = \sigma^2 \delta_{kl}$, where δ_{kl} is the Kronecker symbol and σ is the disturbance variance.

(ii) Apply control voltages on the phase modulators with the positive perturbations and obtain the metric function from the detector $J^+ = J(\boldsymbol{u} + \delta\boldsymbol{u})$, then apply the control voltages with the negative perturbations and gain the metric function $J^- = J(\boldsymbol{u} - \delta\boldsymbol{u})$.

(iii) Calculate the difference between two evaluations of the metric function $\delta J = (J^+ - J^-)/2$.

(iv) Update the control voltages$u_i = u_i + \gamma\delta u_i \delta J$ ($i = 1, 2$), where γ is the update gain; $\gamma > 0$ corresponds to the procedure of maximization in the CBC.

3. Results and discussion

In the experiment, when all preamplifiers are turned on, the output power of the two main amplifiers is measured by the power meter as shown in Fig. 4(a). The total power of the two lasers is about 261 W but limited by the pump power of about 451 W and no evident SBS is observed in the backward laser beams from the optical spectrum analyser. Figure 4(b) shows the spectrum of the first main amplifier, which indicates that the ASE is 25 dB suppressed in the amplifier.

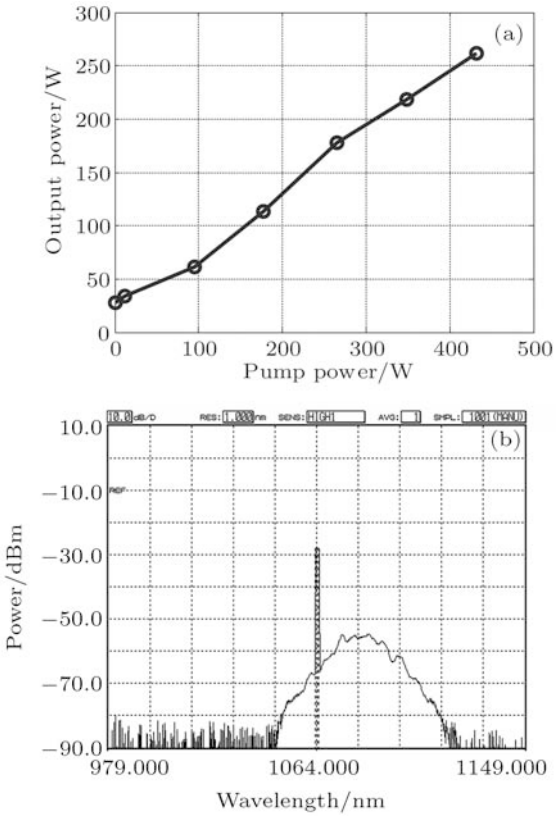


Fig. 4. (a) Output power characteristics of the two main amplifiers, (b) typical spectrum of main amplifier 1.

When the SPGD algorithm is not implemented, the whole system is in open-loop. The metric function (power in the main lobe) fluctuates and the far-field interference pattern keeps shifting due to phase fluctuations in each fibre amplifier. The metric function is fluctuating from 0 to 0.36 V and the mean value is 0.19 V, as presented in the first 22.5 s in Fig. 5(a). The corresponding long-exposure far-field interference pattern is an incoherence one with a fringe visibility of about 0, as shown in Fig. 5(b), where the fringe visibility is defined by the formula $(I_{\max} - I_{\min})/(I_{\max} + I_{\min})$, with $I_{\max}$ and $I_{\min}$ being the maximum intensity and the adjacent minimum of the intensity pattern respectively. When the SPGD algorithm is implemented and the whole system is in closed-loop, γ is taken to be 1.2 and σ is taken to be 0.15, the far-field interference pattern at the observing plane is clear and steady. The dependence of J on time is larger than 0.3 V for most of the time. The mean value is about 0.32 V, which is 1.68 times of that value when the system is in open-loop, as presented in the last 22.5 s in Fig. 5(a). In closed-loop, the intensity pattern at the observing plane is clear and steady, the corresponding long-exposure interference pattern is a coherent one with visibility of about 0.62, as shown in Fig. 5(c). Moveover, a residual phase error is computed to be less than $\lambda/10$ using the expression.[23]

$$\Delta\phi_{\rm rms} = 2\sqrt{\frac{\Delta J_{\rm rms}}{J_{\max}}}, \tag{1}$$

where $J(t)$ is the metric function evolution in closed-loop.

Scaling the system up to higher power can be expected by increasing the power per fibre chain and adding the number of laser channels. The channel number of the system can be extended to $N = F/10f_N$ according to the update rate F of the SPGD controller and the phase noise frequency f_N, while detailed analysis is shown as follows. In statistical meaning, the iterative time k is about $k = 5N - 10N$ when a system metric function evolves from the initialization to the extremum,[18] where N is the channel number used in CBC. The time for a system metric function evolves from the initialization to the extremum is k/F and the control bandwidth of the controller is computed by F/k. Let $k = 10N$ for simplicity, the control bandwidth of the SPGD controller is $F/10N$. Therefore, the channel number N should be less than $F/10f_N$. For the controller with an update rate of 100 kHz, if

the phase noise frequency is about 1000 Hz, then the channel number is $N < (F/10f_N) = 10$. In other words, the channel number can be extended to 10 when the phase noise frequency is about 1000 Hz and the update rate of the SPGD controller is 100 kHz. In order to increase the channel number, one should increase the update rate of the controller and reduce the phase noise of the system.

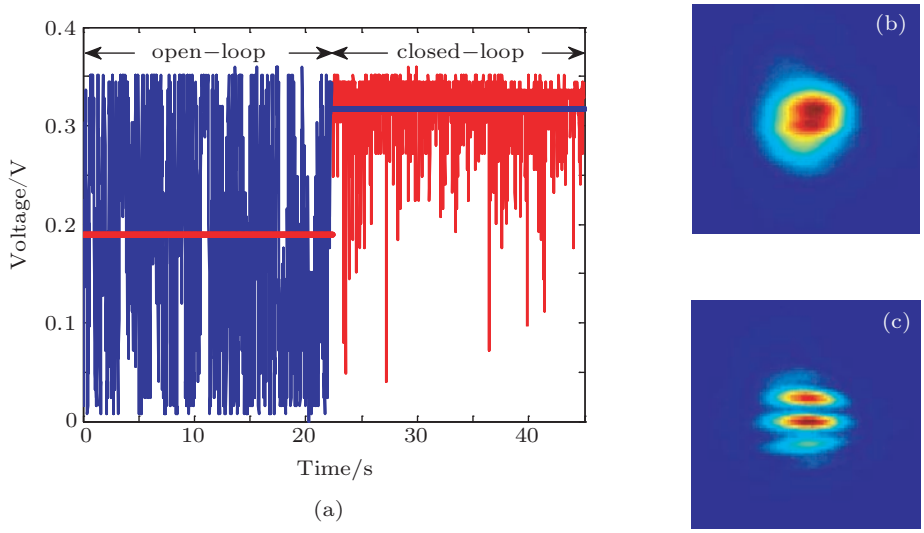


Fig. 5. (colour online) Experimental results: (a) metric function from open-loop to closed-loop, (b) long exposure interference pattern for open-loop, and (c) that for closed-loop.

4. Conclusions

We have demonstrated the CBC of two high-power amplifier chains with a total power of 260 W by using the SPGD algorithm. A 150 MHz linewidth fibre laser is introduced in the amplifier chain to mitigate the SBS and improve the power of amplifiers. Compact high-power amplifier chains are built, when seeded by a 150 MHz linewidth laser, and the system can scale the power from 10 mW to 130 W without any SBS in each amplifier chain. Despite the perturbations of the environment, the visibility of the interference pattern is increased from 0 to 0.62 and the phase residual error is less than $\lambda/10$ when the system evolves from open-loop to closed-loop. Scaling the system to higher power can be expected by increasing the power per fibre chain and adding the number of laser channels.

References

[1] He B, Lou Q, Zhou J, Dong J, Wei Y, Xue D, Qi Y, Su Z, Li L and Zhang F 2006 *Opt. Express* **14** 2721

[2] Peng Q, Sun Z, Chen Y, Guo L, Bo Y, Yang X and Xu Z 2005 *Opt. Lett.* **30** 1485

[3] Li J F, Duan K L, Wang Y S, Zhao W and Guo Y K 2008 *IEEE Photon. Tech. Lett.* **20** 888

[4] Shay T M, Benham V, Bake J T, Sanchez A D, Pilkington D and Lu A C A 2007 *IEEE J. Sel. Top. Quantum Electron.* **13** 480

[5] Wang X L, Zhou P, Ma Y X, Ma H T, Xu X J, Liu Z J and Zhao Y J 2010 *Acta Phys. Sin.* **59** 5474 (in Chinese)

[6] Zhou Pu, Ma Y X, Wang X L, Ma H T, Xu X J and Liu Z J 2010 *Chin. Phys.* B **19** 024207

[7] Liu L, Vorontsov M A, Polnau E P, Weyrauch T and Leonid A B 2007 *Proc. SPIE* **6708** 67080K

[8] Wang X L, Zhou P, Ma Y X, Ma H T, Xu X J, Liu Z J and Zhao Y J 2010 *Chin. Phy.* B **19** 094202

[9] Goodno G D, Mcnaught S J, Rothenberg J E, Mccomb T S, Thielen P A, Wickham M G and Weber M E 2010 *Opt. Lett.* **35** 1542

[10] Limpert J, Röser F, Klingebiel S, Schreiber T, Wirth C, Peschel T, Eberhardt R and Tünnermann A 2007 *IEEE J. Sel. Top. Quantum Electron.* **13** 537

[11] Jeong Y, Nilsson J, Sahu J K, Payne D N, Horley R, Hickey L M B and Turner P W 2007 *IEEE J. Sel. Top. Quantum Electron.* **13** 546

[12] Dawson J W, Messerly M J, Beach R J, Shverdin M Y, Stappaerts E A, Sridharan A K, Pax P H, Heebner J E, Siders C W and Barty C P J 2008 *Opt. Express* **16** 13240

[13] Bellanger C, Paurisse M, Brignon A, Colineau J, Huignard J P, Hanna M, Druon F and Georges P 2010 *Lasers and Electro-Optics (CLEO) and Quantum Electronics and Laser Science Conference (QELS)* p. 1

[14] Goodno G D, Asman C P, Anderegg J, Brosnan S, Cheung E C, Hammo D, Injeyan H, Komine H, Long W H, Jr Mcclellan M, Mcnau S J, Redmond S, Simpson R, Sollee J, Weber M, Weiss S B and Wickham M 2007 *IEEE J. Sel. Top. Quantum Electron.* **13** 460

[15] Jolivet V, Bourdon P, Bennai B, Lombard L, Goular D, Pourtal E, Canat G, Jaouen Y, Moreau B and Vasseur O 2009 *IEEE J. Sel. Top. Quantum Electron.* **15** 257

[16] Shay T M, Benham V, Baker J T, Sanchez A D, Pilkington D and Lu C A 2007 *IEEE J. Sel. Top. Quantum Electron.* **13** 480

[17] Vorontsov M A, Weyrauch T, Beresnev L A, Carhart G W, Liu L and Aschenbach K 2009 *IEEE Journal of Selected Topics in Quantum Electronics* **15** 269

[18] Zhou P, Liu Z J, Wang X L, Ma Y X, Ma H T, Xu X J and Guo S F 2009 *IEEE J. Sel. Top. Quantum Electron.* **15** 248

[19] Vorontsov M 2005 *Proc. SPIE* **5895** 589501

[20] Zhou P, Ma Y X, Wang X L, Ma H T, Wang J H, Xu X J and Liu Z J 2009 *Appl. Opt.* **48** 6537

[21] Zhou P, Wang X, Ma Y, Ma H and Liu Z 2010 *Opt. Lett.* **35** 950

[22] Wang X L, Ma Y X, Zhou P, Ma H T, Li X, Xu X J and Liu Z J 2009 *Laser Phys.* **19** 984

[23] Lombard L, Azarian A, Cadoret K, Bourdon P, Goular D, Canat G, Jolivet V, Jaouën Y and Vasseur A O 2011 *Opt. Lett.* **36** 523